CIVIL ENGINEERING JOURNAL

Article no. 10

THE CIVIL ENGINEERING JOURNAL 1-2025

STATIC PERFORMANCE ANALYSIS OF PRESTRESSED Π-TYPE BEAM CABLE-STAYED BRIDGE CABLE DAMAGE

Dandan Hu

School of Civil and Architectural Engineering, Harbin University, No.109 Zhongxing Road, Harbin, Heilongjiang Province, China; Hardandan@163.com

Received: 11.04.2024

Received in revised form: 05.12.2024

Accepted: 17.01.2025

ABSTRACT

With the increasing span of cable-stayed bridges, the self-weight of the structure accounts for a large proportion. The π-type beam, due to its small cross-sectional area, can significantly reduce the self-weight and cost. It is suitable for double-cable surface system cable-stayed bridges and has therefore experienced rapid development. This paper takes a prestressed π-type beam cable-stayed bridge in China as an engineering example, and focuses on the overall and local parameter sensitivity of the structure, as well as the force characteristics under cable damage. The main factors causing cable damage in prestressed π-type beam cable-stayed bridges are analyzed, and the selection of elastic modulus as the damage variable is determined. Based on the finite element model analysis of the actual bridge, different cable damage simulations are selected to analyze the static variations of the main beam and cables caused by single-side, symmetrical, and asymmetrical cable damage, as well as the dynamic variations of the overall bridge. It significantly affects the vertical displacement of the short main span main beam. When the short cable is damaged 100%, the maximum deflection of the main beam can reach up to 5.29 mm. when the medium cable is damaged 100%, the maximum deflection of the main beam can reach up to 17.87 mm. This analysis provides a reference for the mechanical performance analysis of prestressed π-type beam cable-stayed bridges under similar cable damage conditions in the future.

KEYWORDS

Cable-stayed bridge, π-shaped beam, Finite element analysis, Static performance

INTRODUCTION

A cable-stayed bridge is a large-span statically indeterminate structural system composed of towers, beams, and cables. Currently, both domestic and foreign cable-stayed bridges often adopt a cable-dense system [1-3]. Due to the excellent lateral force performance and large flexural rigidity of the closed box section main beam, it is widely used in various forms of cable-stayed bridges. In order to enhance the wind resistance, inclined webs are often used, which also increase the construction difficulty. Due to practical needs and the maturity of construction techniques, the span

of cable-stayed bridges continues to increase, resulting in an increasing proportion of the structure's self-weight to the applied load. In response to this, bridge designers have proposed the use of a π-shaped main beam section to reduce the self-weight of the main beam [4-6].

Currently, research on prestressed π-type beam cable-stayed bridges has mainly focused on the optimization of cable forces, both domestically and internationally, while studies on the effects of parameters on the operational stage of prestressed π-type beam cable-stayed bridges are relatively scarce [7]. The overall structural parameters have a significant impact on cable-stayed bridges, where auxiliary piers, located between the bridge piers and towers, play a supportive role in significantly improving the overall stiffness of cable-stayed bridges and reducing the vertical displacement of the main beam [8-11]. Under live loads, the use of auxiliary piers can effectively reduce the internal forces and limit the vertical displacement of the main beam, while also reducing the negative reactions at the auxiliary piers. This makes it more convenient to provide counterweights for short main spans in cable-stayed bridges with π-shaped beam sections, which is advantageous for the overall structure [12]. Additionally, certain local structural parameters also have a significant impact on cable-stayed bridges. As cable-stayed bridges are large-span statically indeterminate structures, factors such as temperature changes cannot be ignored in their performance analysis [13]. Therefore, conducting in-depth research on the effects of overall and local parameter variations on the structural performance of π-type beam cable-stayed bridges is of great importance for their development [14].

As a critical component of the entire system, the stay cables bear the majority of the load acting on the main beam. However, during daily operation, various factors such as sheath damage, wire corrosion, and vibration fatigue can cause damage to the stay cables to varying degrees. The damage to the stay cables leads to a redistribution of cable forces across the entire bridge and can induce varying levels of deflection in the main beam, directly affecting the service life of the bridge [15-16]. Currently, research on cable damage mainly focuses on integral box girder and other main beam forms of cable-stayed bridges, and there is limited research on the effects of cable damage on π-shaped beam cable-stayed bridges. With the continuous improvement of inspection methods, a series of protective measures have been developed for cable damage. However, these measures cannot guarantee the safe operation of cable-stayed bridges entirely. If the impact of cable damage on the structural performance of π-shaped beam cable-stayed bridges can be studied, it can provide theoretical support for daily maintenance projects of π-shaped beam cable-stayed bridges.

ENGINEERING BACKGROUND

The engineering background of this study is a single-tower cable-stayed bridge with pre-stressed π-shaped beams in Jilin Province, China. The total length of the bridge is 617.06 m, and the span combination is 39.9 m+89.1 m+151 m, with the second span being the main bridge section under investigation. The main bridge adopts an "H" shaped single-tower double-plane cable-stayed bridge with precast concrete (PC) beams. The span combination of the main bridge is 39.9 m + 89.1 m + 151 m. The main bridge structure is a fixed system, with a 2.0 % bidirectional cross slope in the transverse direction, and designed for City-Class A loading. The main tower has a total of 18 pairs of spatial cables arranged in a fan shape. The inclined cables are arranged at a distance of 0.8 m from the edge of the main beam. The layout of the pre-stressed π-shaped beam cable-stayed bridge is shown in Figure 1.

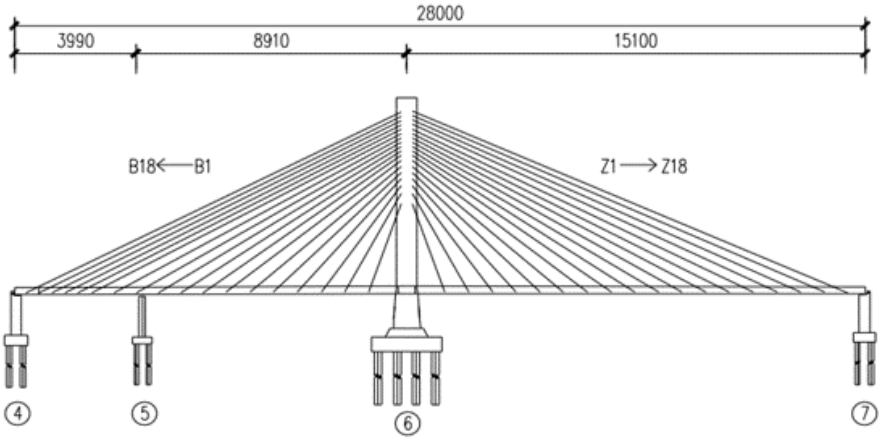

Fig. 1 – Layout diagram of the main bridge

(1) Main beam structure

The main beam adopts a pre-stressed concrete "π" shaped cross-section. The width of the main beam section is 26.5 m, and the height is 2.3 m. It is designed with a bidirectional 2% cross slope. The basic spacing of the transverse beams is 3.9 m, 3.65 m, and 4.25 m. The transverse beams are all equipped with pre-stressed steel hinge lines. The main beam is connected to the main tower using a fixed system, and both the main beam and the transverse beams are made of C55 concrete.

(2) Main tower

The main tower of the cable-stayed bridge adopts an H-shaped main tower. The height of the main tower is 117.318 m. The cross-section of the tower column is a hollow rectangular shape, with a full width of 6.8 m in the middle and upper tower columns longitudinally, and a width of 4.0 m in the transverse bridge direction. The upper part of the lower tower column gradually increases from a width of 6.8 m to a full width of 8.8 m longitudinally, and the width in the transverse bridge direction gradually increases to 7.5 m.

The cross-section of the transverse beam is a hollow rectangular shape. The upper transverse beam has a rectangular cross-section of 6.2 m × 4 m, while the lower transverse beam has a width of 6.4 m and a height ranging from 6 m to 6.27 m. A tower pedestal with a height of 3 m is provided at the top of the main tower's bearing platform. Except for the lower transverse beam, which is made of C55 concrete, the rest of the main tower structures are made of C50 concrete.

(3) Stay cable

The main tower is equipped with a total of 72 stay cables, with each cable spaced at a designed interval of 7.8 m. The cable spacing changes to 7.8 m, 7.3 m, and 4.25 m corresponding to the length variations of the main span's cast-in-place segments. The stay cables are positioned 0.8 m away from the edge of the main beam cross-section. The stay cables are all made of Φ s 15.2 steel strand with a standard strength of 1860 MPa. The stay cable numbering is shown in Figure 1.

FINITE ELEMENT ANALYSIS MODEL

The finite element model of this prestressed π-type girder cable-stayed bridge is established and analyzed using the specialized bridge analysis software, Midas Civil. The main beam and main tower are simulated using 2D beam elements, with section dimensions set to match the actual conditions. The overall finite element model of the prestressed π-type girder cable-stayed bridge

consists of 483 nodes and 399 elements, with 327 beam elements, including 235 main beam elements and 92 main tower elements. There are 72 truss (stay cable) elements that only experience tension. The complete bridge finite element model is shown in Figure 2.

The main beam and main tower are simulated in the cable-stayed bridge using the shared node approach to model the fixed support system. The auxiliary piers and main beam are rigidly connected, and the connection between the stay cable anchorage points, main beam, and main tower is simulated using rigid connections as well. The transverse beams on the main beam and main tower are made of C55 concrete. The lower transverse beam of the main tower, upper tower columns, middle tower columns, lower tower columns, and tower base are made of C50 concrete. The 5# auxiliary pier is made of C40 concrete.

Both longitudinal and transverse prestressing tendons are made of high-strength low-relaxation prestressing strand with a single strand diameter of Φ s 15.2 mm. The standard strength of the strand is 1860 MPa, with an elastic modulus of 1.95×10^5 MPa, and a cross-sectional area of 140 mm^2.

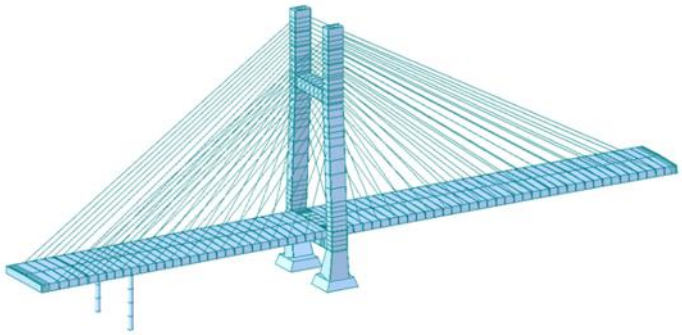

Fig. 2 – The finite element model of the main bridge

STATIC PERFORMANCE ANALYSIS OF THE PRESTRESSED Π-TYPE GIRDER CABLE-STAYED BRIDGE UNDER IDENTICAL DAMAGE CONDITIONS OF STAY CABLES

In order to analyze the influence of stay cable damage on the static performance of the structure, the most deviated stay cable at the furthest point from the main tower is selected from the long, medium, and short cables as a representative stay cable for damage simulation and analysis.

Analysis of the Influence of Static Performance under the Same Level of Damage for Single-side Stay Cables

This section primarily focuses on the analysis of the influence of single-side stay cable damage at the same level of 60% on the static characteristics of the prestressed π-type girder cable-stayed bridge. The load combinations are shown in Table 1.

Tab. 1 - Damage load combination table

Operating conditions	Cable damage	Cable identification
Operating conditions 1	Secondary span and short main span cable damage	B6
Operating conditions 2	Secondary span and short main span mid-cable damage	B12
Operating conditions 3	Secondary span and short main span long-cable damage	B18
Operating conditions 4	Long main span short-cable damage	Z6
Operating conditions 5	Long main span mid-cable damage	Z12
Operating conditions 6	Long main span long-cable damage	Z18

Using the Midas Civil software, the six working conditions mentioned above can be simulated by changing the elastic modulus of the inclined cables. The analysis will provide the internal force variation of each cable and the vertical displacement variation of the main beam under each working condition, as shown in Figure 3 and Figure 4. The maximum displacement variation values can be found in Table 2. In the cable force variation graph, negative values represent the inclined cable condition without any damage.

In comparison with the cable forces, for this working condition, the cable force of the inclined cable is reduced. A positive value represents the internal force of the inclined cable in comparison with the undamaged cable condition, and for this working condition, the cable forces of the inclined cable are increased. In the vertical displacement variation graph of the main beam, a positive value indicates that the point on the main beam moves upward after cable damage, while a negative value indicates that the point moves downward compared to the situation before cable damage.

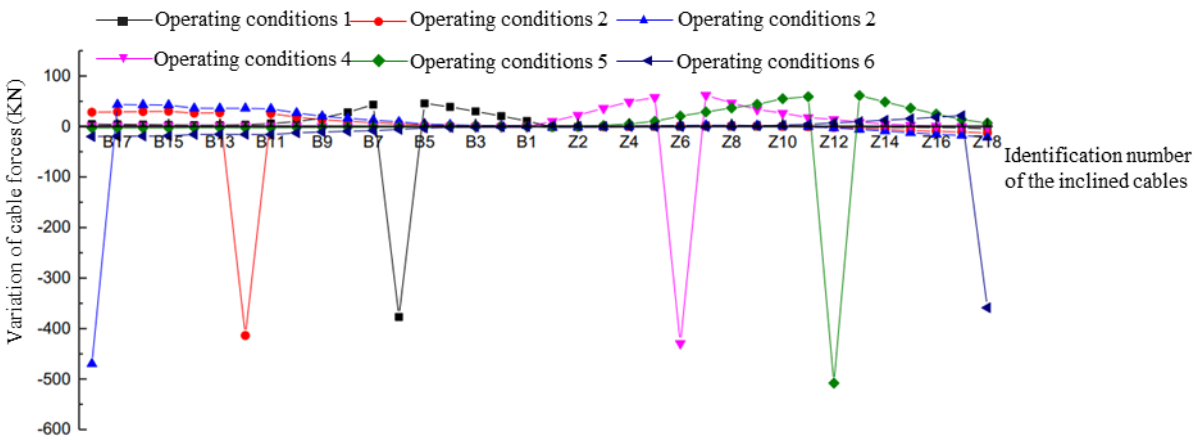

Fig. 3 – Graph of cable force variation for damaged inclined cables

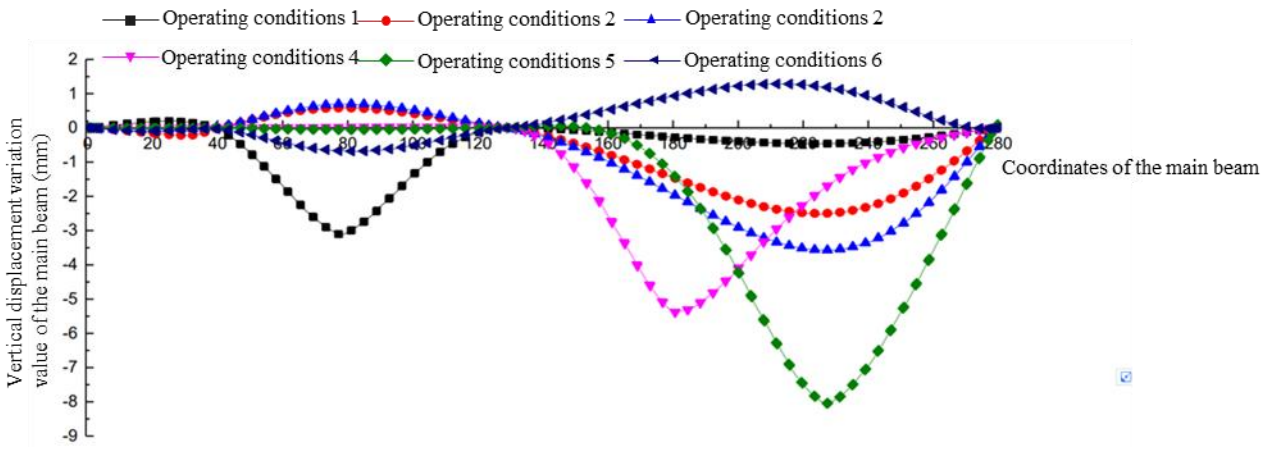

Fig. 4 – Graph of vertical displacement variation of the main beam with damaged inclined cables

From Figure 3, it can be observed that for 60% damage to the inclined cables on auxiliary and short main spans, the decrease in cable force variation value around the damaged cable decreases gradually with increasing distance. However, in the case of damage to the short and medium cables, the aforementioned decrease trend is more prominent, indicating that the excessive tensile force after damage to the long cable is not evenly distributed to the surrounding inclined cables. In the case of 60% damage to the inclined cable on the long main span, the damage to the long cable has minimal impact on other inclined cables, and the excessive tensile force after damage is distributed to the surrounding inclined cables to a similar extent when damage occurs to the short and medium cables.

Overall, the damage to the inclined cables has limited impact on the surrounding cables, with only a significant effect on approximately 24 nearby cables. The influence on distant cables is relatively small. When the inclined cables are damaged, there is a change in cable force for the damaged cables.

The decrease in value is most pronounced, and the cable forces on both sides of the damaged inclined cables will increase to varying degrees. The magnitude of the increase in cable force will gradually decrease with increasing distance from the damaged inclined cables, but there will be a certain degree of decrease in the cable forces on the opposite side inclined cables.

From Figure 4 and Table 2, it can be concluded that for the auxiliary span, the impact on the vertical displacement can be considered negligible due to its small span and the occurrence of cable damage throughout the bridge. For the short main span, there is only a noticeable deflection in scenarios 1 and 6 compared to the undamaged condition, with a maximum deflection of 3.11 mm observed in scenario 1. However, in scenarios 5 and 6, an upward deflection is observed at various points compared to the undamaged condition, with a similar level of impact on the short main span in both scenarios. For the long main span, scenario 5 shows a significant impact on the vertical displacement, with a peak value of up to 8.05 mm.

Generally speaking, the closer the damaged inclined cable is to the location of maximum bending moment on the main beam, the greater the impact on the vertical displacement of the main span.

Tab. 2 - Table of maximum displacement changes

Operating conditions	Operating conditions 1	Operating conditions 2	Operating conditions 3	Operating conditions 4	Operating conditions 5	Operating conditions 6
Maximum positive displacement (mm)	0.2	0.58	0.7	0.03	0.11	1.28
Maximum negative displacement (mm)	3.11	2.5	3.57	5.38	8.05	0.68

Analysis of the Influence of Symmetric Inclined Cables with the Same Level of Damage on Static Performance

The main study focuses on the analysis of the influence of symmetric inclined cables with the same level of damage (60%) on the static characteristics of prestressed π-type girder cable-stayed bridges. The combination of working conditions is shown in Table 3.

Tab. 3 - Table of damage condition combinations

Operating conditions	Cable damage combinations	Slant cable numbering
Operating conditions 7	Damage to four short cables on the left and right sides of the main tower	B6+ Z6
Operating conditions 8	Damage to four intermediate cables on the left and right sides of the main tower	B12+ Z12
Operating conditions 9	Damage to four long cables on the left and right sides of the main tower	B18+ Z18

Using the Midas Civil software, the three scenarios mentioned above were simulated for cable damage by modifying the elastic modulus of the slant cables. The analysis results include the variation of internal forces in each cable and the vertical displacement of the main beam as shown in Figure 5 and Figure 6. The maximum displacement variations are listed in Table 4. In the cable force variation graphs, negative values represent a decrease in cable force compared to the intact condition of the cables, indicating a decrease in cable force for that scenario. Positive values represent an increase in cable force compared to the intact condition of the cables, indicating an increase in cable force for that scenario. In the vertical displacement variation graph of the main beam, positive values indicate an upward movement of the corresponding point of the main beam after cable damage, while negative values indicate a downward movement compared to the pre-damage condition of the cable.

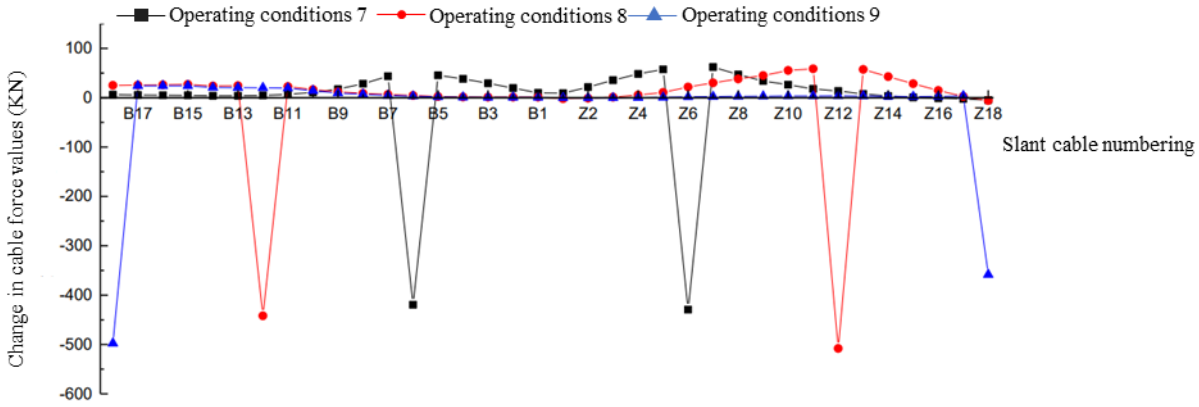

Fig. 5 – Symmetric cable force variation diagram for damaged inclined cables

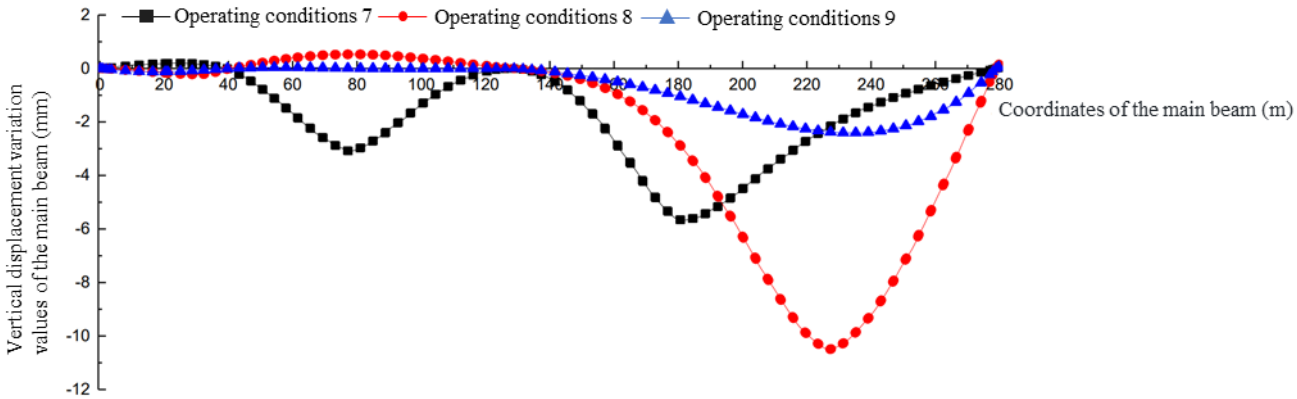

Fig. 6 – Symmetric inclined cable damaged main beam vertical displacement variation diagram

According to Figure 5, it can be concluded that the largest variation in cable force occurs when damage is present in the diagonal cables of auxiliary spans and short main spans, with a decrease of 497 kN and a variation range of 6.87%. Similarly, for the diagonal cables in long main spans, the cable force variation is most significant, with a decrease of 508 kN and a variation range of 12.9%.

According to Figure 6 and Table 4, it can be concluded that for the auxiliary spans, the influence of symmetric cable damage on the vertical displacement of the main beam can be negligible. For the short main spans, the vertical displacement is most significantly affected by symmetric short cable damage, with a maximum variation range of 3.08 mm. Similarly, for the long main spans, the symmetric middle cable damage has the most significant impact, with a maximum variation range of 10.50 mm. Moreover, the peak variation in displacement is close to the location of the damaged cable in the long main span.

Tab. 4 - Damage load combination table

Operating conditions	Maximum positive displacement (mm)	Maximum negative displacement (mm)
Operating conditions 7	0.20	5.66
Operating conditions 8	0.53	10.50
Operating conditions 9	0.07	2.41

Analysis of the Influence of Static Performance under the Same Degree of Damage for Asymmetrical Inclined Cables

The main study focuses on the analysis of the effects of asymmetric inclined cables with pre-stressed π-type beam cable-stayed bridge on the static characteristics of the cable-stayed bridge under the same damage level of 60%. The combinations of damage conditions are listed in Table 5.

Tab. 5 - Combination of damage conditions

Operating conditions	Cable damage	Diagonal cable number
Operating conditions 10	Damage to the left short cable and right middle cable on the main tower	B6+ Z12
Operating conditions 11	Damage to the short cable on the left side and the long cable on the right side of the main tower	B6+ Z18
Operating conditions 12	Damage to the middle cable on the left side and the short cable on the right side of the main tower	B12+ Z6
Operating conditions 13	Damage to the middle cable on the left side and the long cable on the right side of the main tower	B12+ Z18
Operating conditions 14	Damage to the long cable on the left side and the short cable on the right side of the main tower	B18+ Z6
Operating conditions 15	Damage to the long cable on the left side and the middle cable on the right side of the main tower	B18+ Z1

Using the Midas Civil software, the damage simulation of the 6 working conditions through changing the elastic modulus of the inclined cables is conducted. The variations in cable forces and vertical displacements of the main beam under each working condition are shown in Figure 8 and Figure 8. The maximum displacement change values are listed in Table 6. In the cable force variation graph, negative values indicate a decrease in cable force compared to the intact condition, while positive values indicate an increase in cable force. In the vertical displacement variation graph of the main beam, positive values indicate an upward movement of the point after cable damage, while negative values indicate a downward movement compared to the pre-damage state.

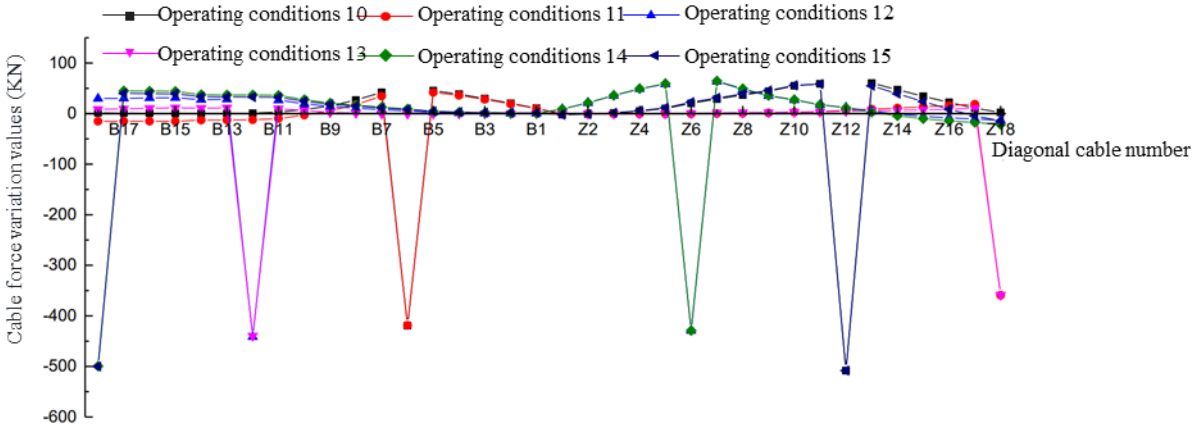

Fig. 7 – Asymmetric inclined cable damage cable force variation graph

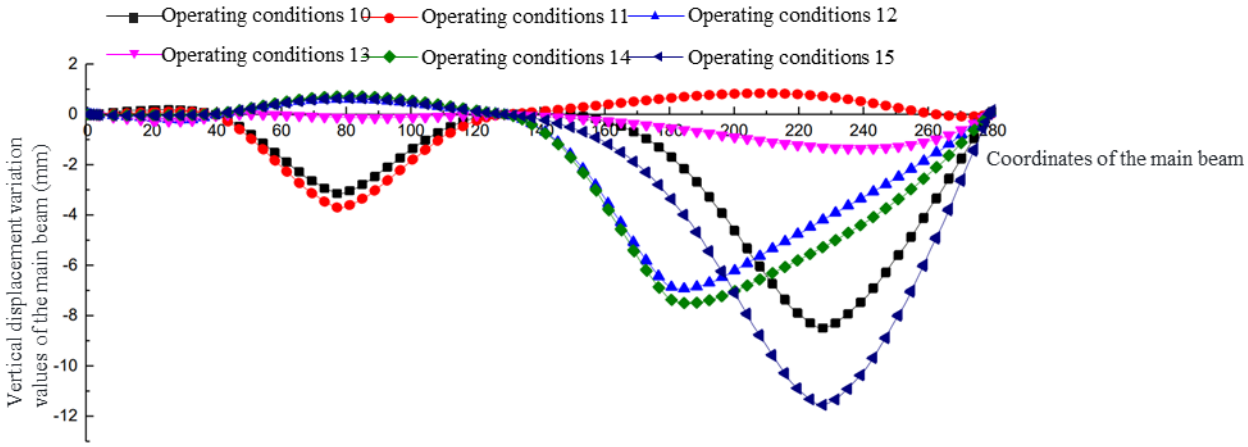

Fig. 8 – Graph showing the variation of vertical displacement of the main beam due to asymmetric inclined cable damage

From Figure 7, it can be concluded that when asymmetric damage occurs in the inclined cables of the entire bridge, the increase in cable force will not be affected by the damage to the cables on the other side of the main tower. It is essentially equivalent to a combination of cable force increment values under the condition of damage to a single side of the cables.

From Figure 8 and Table 6, it can be concluded that for the auxiliary span, regardless of the combination of asymmetric damage in the bridge cables, the impact on its main beam vertical displacement can be negligible. However, for the short main span, load case 11 has the most significant influence on its main beam vertical displacement, with a variation value of 3.71 mm. Similarly, for the long main span, load case 15 has the most significant influence on its main beam vertical displacement, with a variation value of 11.55 mm.

STATIC PERFORMANCE ANALYSIS OF PRESTRESSED Π-SHAPED BEAM CABLE-STAYED BRIDGES UNDER DIFFERENT STAY CABLE DAMAGE CONDITIONS

Considering the selection of stay cables corresponding to load cases 7, 8, and 9, the impact of different levels of symmetric stay cable damage on cable-stayed bridges is studied. The damage levels of the stay cables are set at 20%, 40%, 60%, 80%, and 100%, respectively, and compared

with the intact condition for comparative analysis. The load case numbers corresponding to the damage levels are indicated in Table 6.

Tab. 6 - Damage condition combination table

Operating conditions	Stay Cable Damage Combination	Stay Cable Identification Number
Operating conditions 16	Symmetrical Short Cable Damage 20%	B6+ Z6
Operating conditions 17	Symmetrical Short Cable Damage 40%	B6+ Z6
Operating conditions 18	Symmetrical Short Cable Damage 60%	B6+ Z6
Operating conditions 19	Symmetrical Short Cable Damage 80%	B6+ Z6
Operating conditions 20	Symmetrical Short Cable Damage 100%	B6+ Z6
Operating conditions 21	Symmetrical Middle Cable Damage 20%	B12+ Z12
Operating conditions 22	Symmetrical Middle Cable Damage 40%	B12+ Z12
Operating conditions 23	Symmetrical Middle Cable Damage 60%	B12+ Z12
Operating conditions 24	Symmetrical Middle Cable Damage 80%	B12+ Z12
Operating conditions 25	Symmetrical Middle Cable Damage 100%	B12+ Z12
Operating conditions 26	Symmetrical Long Cable Damage 20%	B18+ Z18
Operating conditions 27	Symmetrical Long Cable Damage 40%	B18+ Z18
Operating conditions 28	Symmetrical Long Cable Damage 60%	B18+ Z18
Operating conditions 29	Symmetrical Long Cable Damage 80%	B18+ Z18
Operating conditions 30	Symmetrical Long Cable Damage 100%	B18+ Z18

Using the Midas Civil software, a simulation of stay cable damage was conducted for the aforementioned 15 load cases by varying the elastic modulus of the stay cables. The analysis provides the variation of internal forces in each cable and the vertical displacement of the main beam for each load case, as shown in Figure 9 - Figure 14. In the cable force variation plot, negative values indicate a decrease in cable force compared to the undamaged condition, while positive values

indicate an increase in cable force compared to the undamaged condition. In the main beam vertical displacement plot, positive values represent an upward movement of the main beam at that point after cable damage, while negative values represent a downward movement compared to the pre-damage condition of the cables.

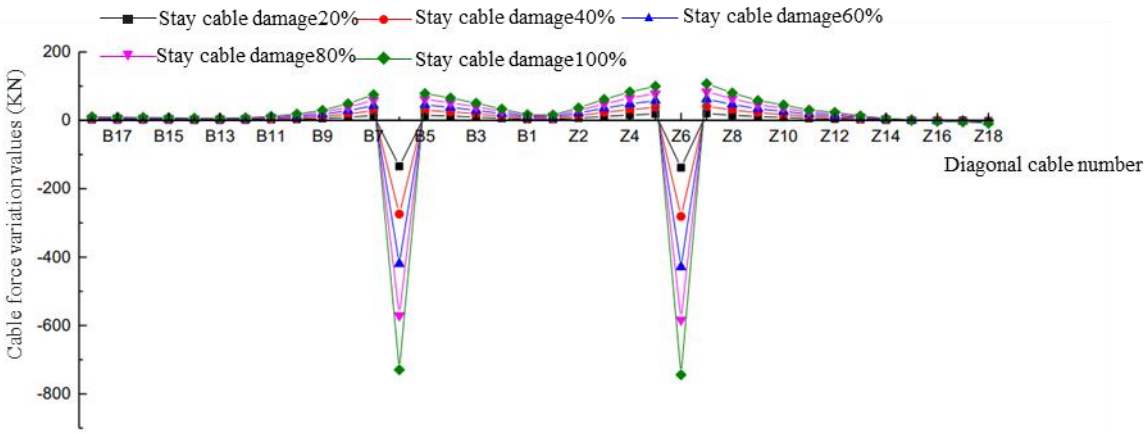

Fig. 9 – Symmetrical short cable damage - cable force variation plot

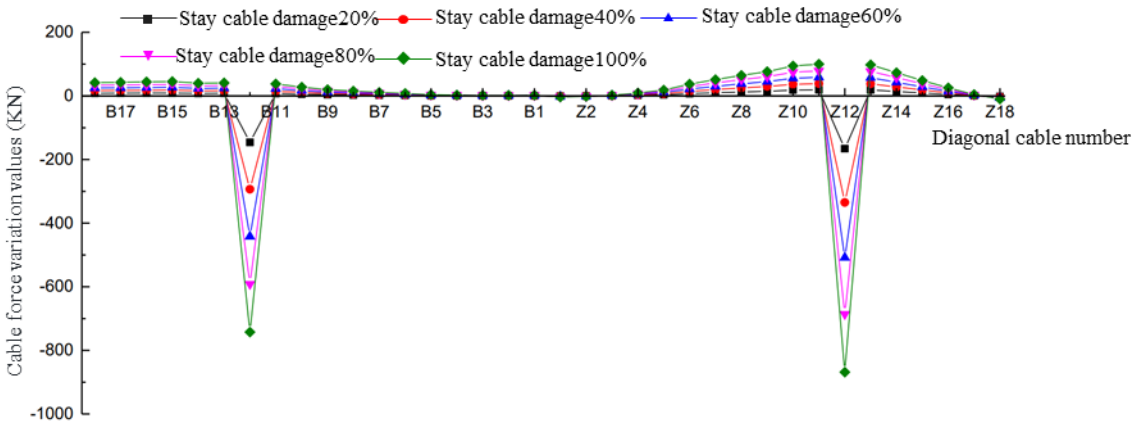

Fig. 10 – Symmetrical medium cable damage - cable force variation plot

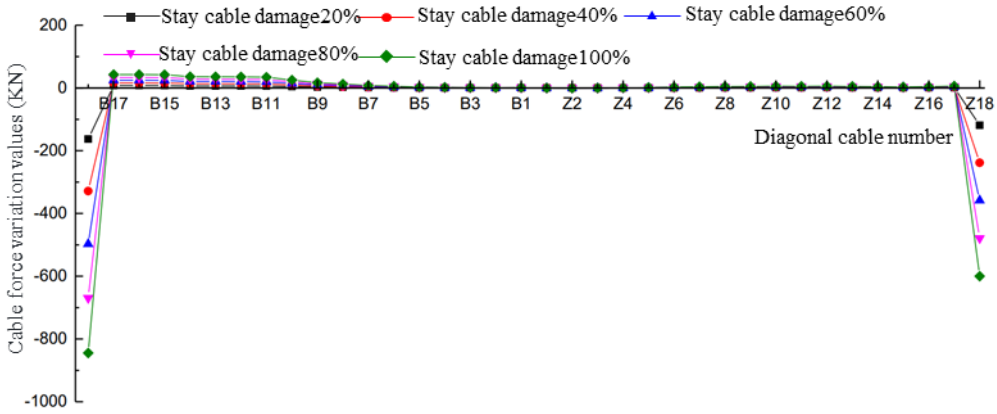

Fig. 11 – Symmetrical long cable damage - cable force variation plot

From Figure 10 - Figure 12, it can be concluded that as the degree of damage to the same cable location increases, the reduction in internal force of the damaged cable becomes more significant. At the same time, the different levels of damage to the cables have a similar trend in redistributing the internal forces of the π-type cable-stayed bridge. Cables closer to the damaged cable experience larger changes in internal forces, whereas cables farther away from the damaged cable generally do not exhibit significant changes.

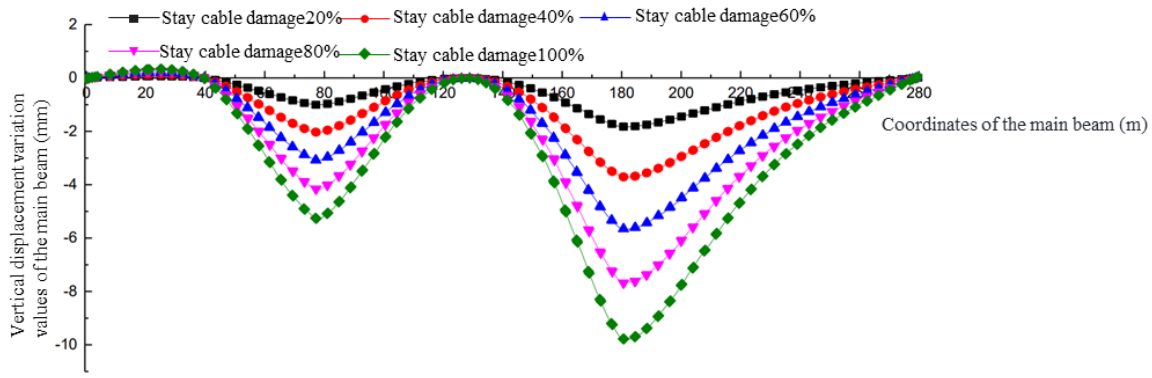

Fig. 12 – Symmetrical short cable damage - vertical displacement variation plot of the main beam

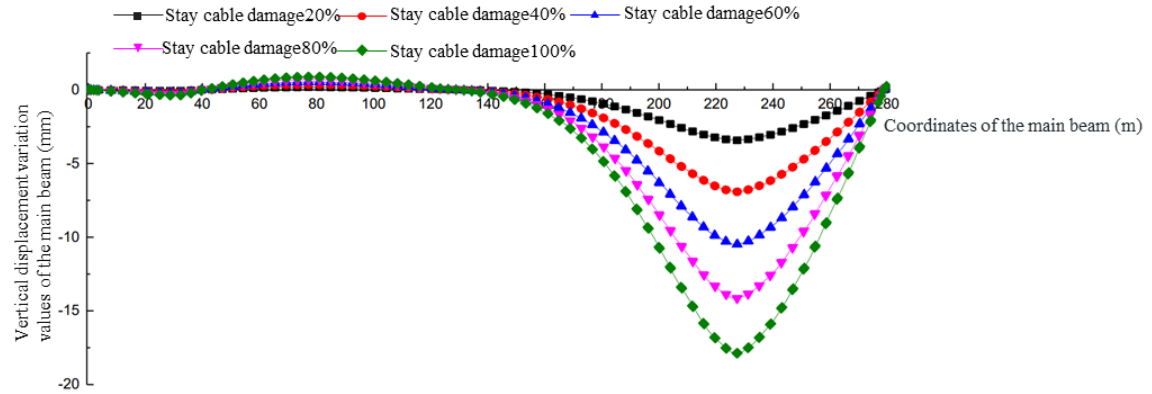

Fig. 13 – Symmetrical medium cable damage - vertical displacement variation plot of the main beam

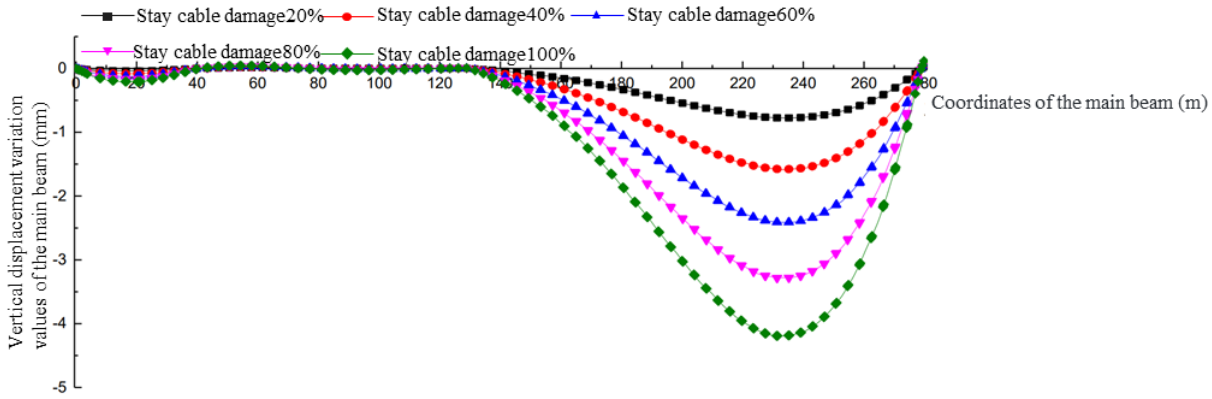

Fig. 14 – Symmetrical long cable damage - vertical displacement variation plot of the main beam

Based on Figure 12 - Figure 14, it can be observed that for symmetrical cable damage at any level, it has minimal impact on the vertical displacement of the auxiliary span main beam. However, in the case of symmetrical short cable damage, it significantly affects the vertical displacement of the short main span main beam. When the short cable is damaged 100%, the maximum deflection of the main beam can reach up to 5.29 mm. Symmetrical cable damage leads to deflections at various points along the long main span main beam, especially when the medium cable is damaged 100%, the maximum deflection of the main beam can reach up to 17.87 mm. In general, for damage to the same cable location, the greater the extent of cable damage, the greater the impact on the vertical displacement of the main beam. However, the trend of vertical displacement remains the same. The maximum deformation of the main beam occurs at the location of the damaged cable. The vertical displacement of the main beam is greater closer to the damaged cable and smaller farther away from it.

CONCLUSION

This paper takes a prestressed π-type beam cable-stayed bridge in China as an engineering example, and focuses on the overall and local parameter sensitivity of the structure, as well as the force characteristics under cable damage. The main factors causing cable damage in prestressed π-type beam cable-stayed bridges are analyzed, and the selection of elastic modulus as the damage variable is determined. Conclusions are as follows:

(1) After damage occurs to symmetric or asymmetric cable-stays, the peak impact on cable forces is observed at the location of the damaged cable itself. The force value of the damaged cable decreases significantly, while the surrounding cable forces increase and exhibit a decreasing trend towards both sides. However, when damage occurs to a single-side cable-stay, the cable force on the other side of the main tower may decrease to some extent, but the level of impact can be considered negligible.

(2) For the same level of damage, the trend and extent of the influence on cable forces for symmetric cable-stays and single-side cable-stays are generally similar. It significantly affects the vertical displacement of the short main span main beam. When the short cable is damaged 100%, the maximum deflection of the main beam can reach up to 5.29 mm. when the medium cable is damaged 100%, the maximum deflection of the main beam can reach up to 17.87 mm.

(3) Due to the presence of the auxiliary pier, whether symmetric or asymmetric cable damage occurs, the impact on the linearity of the main span girder is much greater than the impact on the linearity of the auxiliary span and short main span. When damage occurs to the long cables of the auxiliary span, short main span, or the medium cable of the main span, it has the most adverse effect on the vertical displacement of the main beam and requires careful observation during the operation of the bridge. The closer the damaged cable is to the mid-span of the respective span, the greater its influence on the vertical displacement of that span. Within the elastic working range, different levels of damage.

REFERENCES

[1] Bai H, Li R, Xu G, et al. Aerodynamic performance of Π-shaped composite deck cable-stayed bridges including VIV mitigation measures[J]. Journal of Wind Engineering and Industrial Aerodynamics, 2021, 208: 104451.

[2] Zhang K, Li D, Xue X. Process monitoring and terminal verification of π–section girder cable-stayed bridge[J]. International Journal of Building Pathology and Adaptation, 2023.

[3] Mandić R, Hadži-Niković G, Ćosić S. Investigation of the behavior of the cable-stayed bridge under test load[J]. Geofizika, 2011, 28(1): 145-160.
[4] Cho S, Yim J, Shin S W, et al. Comparative field study of cable tension measurement for a cable-stayed bridge[J]. Journal of Bridge Engineering, 2013, 18(8): 748-757.
[5] Soneji B B, Jangid R S. Influence of soil–structure interaction on the response of seismically isolated cable-stayed bridge[J]. Soil Dynamics and Earthquake Engineering, 2008, 28(4): 245-257.
[6] El Ouni M H, Kahla N B, Preumont A. Numerical and experimental dynamic analysis and control of a cable stayed bridge under parametric excitation[J]. Engineering Structures, 2012, 45: 244-256.
[7] Wen J, Han Q, Xie Y, et al. Performance-based seismic design and optimization of damper devices for cable-stayed bridge[J]. Engineering Structures, 2021, 237: 112043.
[8] Li C, Li H N, Hao H, et al. Seismic fragility analyses of sea-crossing cable-stayed bridges subjected to multi-support ground motions on offshore sites[J]. Engineering Structures, 2018, 165: 441-456.
[9] Soneji B B, Jangid R S. Passive hybrid systems for earthquake protection of cable-stayed bridge[J]. Engineering structures, 2007, 29(1): 57-70.
[10] Liu Z, He F, Yan A, et al. Mechanism and Aerodynamic Countermeasures of Vortex-Induced Vibration of a Cable-Stayed Bridge with Narrow Π-Shaped Girder Sections[J]. Journal of Bridge Engineering, 2023, 28(12): 04023090.
[11] Hou N, Sun L, Chen L. Cable reliability assessments for cable-stayed bridges using identified tension forces and monitored loads[J]. Journal of Bridge Engineering, 2020, 25(7): 05020003.
[12] Kang H, Su X, Pi Z. Planar nonlinear dynamic analysis of cable-stayed bridge considering support stiffness[J]. Nonlinear Dynamics, 2022, 107(2): 1545-1568.
[13] Ma C, Duan Q, Liao H. Experimental investigation on aerodynamic behavior of a long span cable-stayed bridge under construction[J]. KSCE Journal of Civil Engineering, 2018, 22: 2492-2501.
[14] Wang R, Xu Y, Li J. Transverse seismic behavior studies of a medium span cable-stayed bridge model with two concrete towers[J]. Journal of Earthquake Engineering, 2017, 21(1): 151-168.
[15] Larsen A, Larose G L. Dynamic wind effects on suspension and cable-stayed bridges[J]. Journal of Sound and Vibration, 2015, 334: 2-28.
[16] Cong Y, Kang H. Planar nonlinear dynamic behavior of a cable-stayed bridge under excitation of tower motion[J]. European Journal of Mechanics-A/Solids, 2019, 76: 91-107.